

Flux jumps in irradiated MgB₂ dense samples

E. Verdín

Departamento de Física, Universidad de Sonora, 83000 MÉXICO.

C. Romero, F. Morales, and R. Escudero

*Instituto de Investigaciones en Materiales, Universidad Nacional Autónoma de México,
México Distrito Federal, 04510 MÉXICO.*

E. Adem and J. Rickards

*Instituto de Física, Universidad Nacional Autónoma de México,
04510 MÉXICO.*

A. Durán and D.H. Galván

*CCMC-Universidad Nacional Autónoma de México,
Ensenada B. C. 22800, MÉXICO.*

M.B. Maple

*Department of Physics and Institute of Pure and Applied Physical Sciences, University of California,
San Diego, La Jolla, CA 92093-0411, USA.*

Recibido el 30 de noviembre de 2006; aceptado el 8 de octubre de 2007

This work presents studies of magnetic flux jump instabilities in MgB₂ dense bulk samples irradiated with electrons, protons, and gamma rays. Isothermal magnetization vs magnetic field measurements (M-H) at different temperatures display flux jump instabilities that are strongly dependent on the temperature. Hysteresis loops, below the superconducting transition temperature, allow us to conclude that the different types of irradiation affect the magnetic and electronic properties in different ways. The study was performed in MgB₂ irradiated samples that were compared with pristine ones.

Keywords: MgB₂; flux pinning; hysteresis loop.

Se presenta un estudio de las inestabilidades de fluxones magnéticos en muestras de alta densidad de MgB₂, irradiadas con electrones, protones y rayos gama. Las medidas isotérmicas de la magnetización versus el campo magnético, (M-H) a diferentes temperaturas, muestran inestabilidades en vórtices de flujo magnético que son fuertemente dependientes de la temperatura. Los ciclos de histéresis a temperaturas menores de la temperatura de transición superconductor permitieron concluir que los diferentes tipos de irradiación, afectan en forma diferente a las propiedades magnéticas y electrónicas. El estudio se realizó en muestras de MgB₂ irradiadas, y fueron comparadas con las muestras sin irradiación.

Descriptores: MgB₂; comportamiento de vórtices; histéresis magnética.

PACS: 74.70.AD; 61.80.Hg

1. Introduction

MgB₂ is an interesting material recently discovered that presents superconductivity [1]. This apparently simple binary compound has an electronic density of states formed with s and p electrons alone. It was prepared for the first time in 1953 by Jones and March. Its crystal structure consists of hexagonal alternate layers of B and Mg. The space group is P6/mmm with lattice constants $a=3.086$ Å and $c=3.524$ Å, Fig. 1. Lattice parameters fit the radii of the metal and covalent radius of B, the c/a ratio is close to 1. In general, diborides are non-magnetic, except the Cr and Mn systems. NbB_{2+x} is the other unique superconductor in this diborides family, but this has only 9.8 K [2]. MgB₂ decomposes peritectically, without a liquidus-solidus line; this is the reason why the growth of single crystals is difficult. Various forms of preparation exist; one uses Ta tubes sealed in quartz ampoules calcined at about 950°C. After two hours of heating and once allowed to cool to room temperature, the compound

is formed. Another method is simpler; it uses RF heating in an Ar-H₂ (about 2 - 5 % H₂) atmosphere; the compound may be rapidly formed in about 5 to 20 minutes. The reaction occurs via Mg diffusion into B powders; H₂ prevent Mg oxidation.

Type II superconducting behavior in this compound was discovered in the year 2001 [3], and presents a transition temperature of about 39 K. The electronic characteristics of this compound are: high electronic density of states and strong electron-phonon (e-ph) coupling. In spite of the simpler crystalline structure, the electronic structure is rather complex. It has two band gaps leading to the rather complex electronic behavior [4-6], see Fig. 2. The electronic interaction of the bands that form the superconducting condensate induces the formation of two energy superconducting gaps, a quite unique behavior in this compound; in fact, the two gaps are observed by heat capacity [7] and point contact spectroscopy [8] measurements.

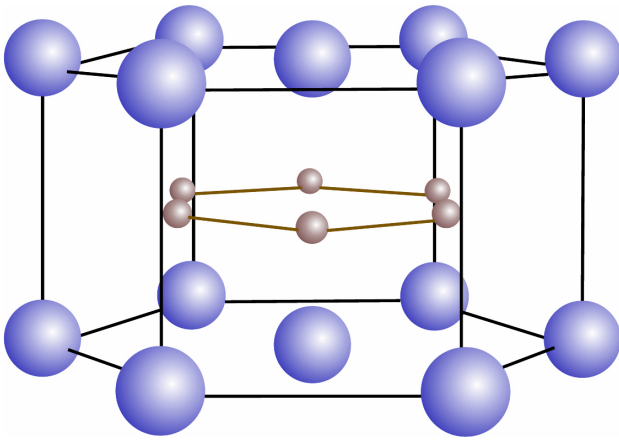


FIGURE 1. Crystal structure of MgB_2 compound showing the Mg and B layers, small spheres represent B atoms

The high transition temperature of this compound can be completely explained by an electron-phonon coupling, which closely follows the BCS predictions. The discovery of this and other superconducting materials above 30 K is a fact that contradicts the 1960-70 theoretical explanation of the impossibility to obtain an electron-phonon mediated superconductor with a transition temperature above 30 K.

The phonon density of states in MgB_2 is formed by one acoustical phonon at 36 meV and four optical phonons at 54, 78, 89, and 97 meV. The e-ph coupling that forms the electronic condensate is the energetic optical phonon at 78 meV; this is the E_{2g} phonon. Studies about other superconducting characteristics of this compound show that the isotopic effect is similar to compounds or alloys with s and p electrons; thus, the exponent of about 0.2, smaller than the canonical value of 0.5, is rather common in s and p electron compounds. The isotopic effect value is mainly due to the Mg atoms. Another important characteristic is the size of the Ginzburg-Landau κ parameter, which is about 26, with H_{C2} close to 15-18 T, and critical current density of about $10^5 - 10^6 \text{ A/cm}^2$.

One last important aspect related to technological applications is that the effect of grain boundaries in this material is almost minimum, without affecting the supercurrent transport, thus enabling it to carry high current densities [9].

Since the discovery of this material, much work has been

performed based on two aspects: one related to the study of the electronic anomalous characteristics, and the other related to the applications. On the application side, but related with the electronic characteristics, studies on thin films [10] and wires [11] show that, in this compound, thermal instabilities and flux jumps affect the current carrying capabilities, as occur in type II superconductors [12]. Experimental studies related to the magnetization with applied magnetic field M-H at different temperatures have found flux jump behavior that is disadvantageous because it reduces the critical current densities, thus limiting the related superconducting applications. Understanding the flux jump mechanism and thermal instabilities is important from the viewpoint of the technical applications.

Magnetization flux jumps are usually associated with thermomagnetic instability of the flux lines (vortices) that penetrate the compound above H_{C1} . Flux vortex motion is a mechanism that dissipates heat. Vortex flux motion provokes a local temperature increase due to Joule heating [13]. This process produces a sudden temperature rise in a tiny sample region, that in turn produces a sudden decrease of the magnetization, which can be seen as a large macroscopic magnetic flux avalanche.

One general method used to control flux avalanche jumps is by means of the introduction of disorder in the crystallographic structure of the material. This can be induced by introducing non-magnetic impurities to produce pair breaking [14]. Other scattering effects, as intraband effects, affect the resistivity, leading to changes on the shape of the upper critical field, exhibiting a different behavior as predicted by BCS [15, 16].

Disorder introduced by doping enhances the intraband and/or interband scattering, but this effect depends on the doping site. However, this disorder can also be produced by structural deformations that form pinning centers in the lattice.

In high temperature superconductors, irradiation by ions, electrons, protons and gammas to produce crystalline disorder and vortex pinning centers have frequently been used. In principle, the physical mechanism is rather simple: energetic particles passing through the material displace atoms from their equilibrium lattice position, creating vacancies and in-

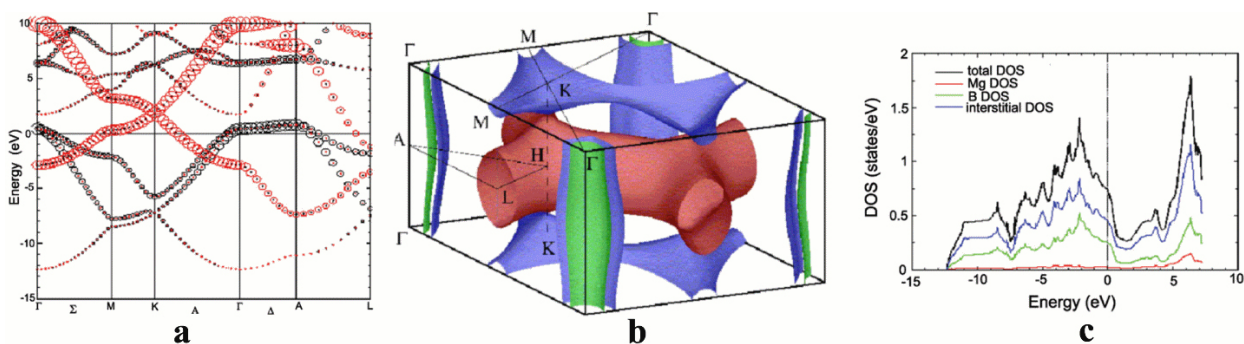


FIGURE 2. Band structure of MgB_2 . a) The band structure in different regions of the reciprocal space. b) The three dimensional Fermi surface. c) The total density of states and the partial density of states for the two atoms [4–6].

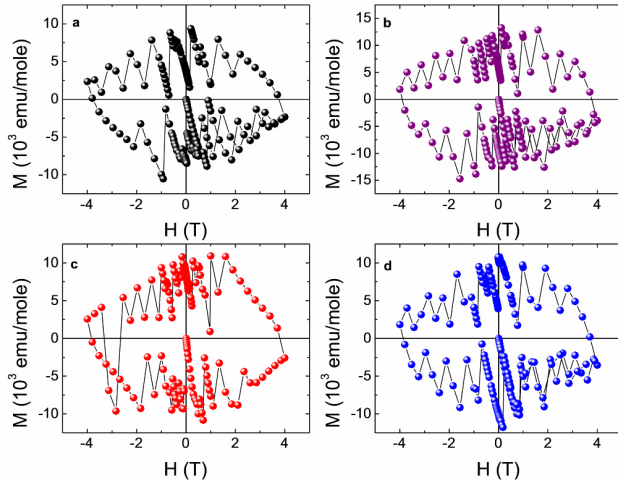


FIGURE 3. Magnetization versus magnetic field hysteresis loops measured in samples of MgB_2 at 2 K. In a) non irradiated, b) irradiated with electrons, c) irradiated with protons and d) irradiated with gammas. Note the high number of magnetic flux avalanches.

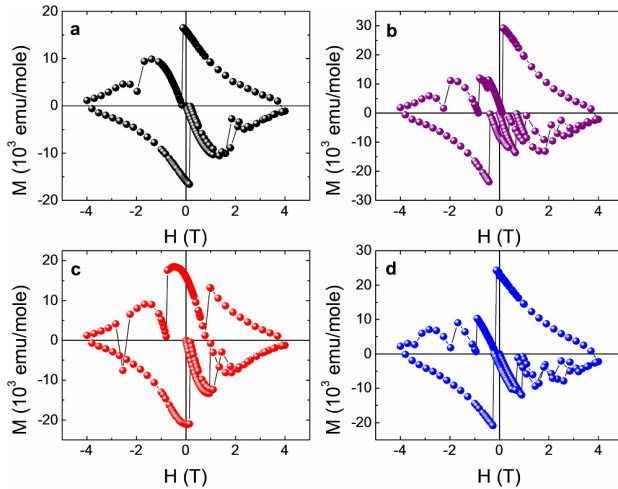


FIGURE 4. Magnetization versus magnetic field hysteresis loops measured in samples of MgB_2 at 10 K. In a) non irradiated, b) irradiated with electrons, c) irradiated with protons, and d) irradiated with gammas. Note that the avalanche number decreases as compared with the measurements at 2 K.

terstitial positions in the lattice; henceforth, in this form, creating pinning centers that inhibit the motion of the vortex lattice. This procedure significantly enhances the critical current density. Another manner to increase the current densities and also the upper critical field can be obtained by nano doping of different compounds. For instance, high critical fields of about 37 T have been obtained by nano-SiC doping. Thus, while defects and grain boundaries could be responsible for the flux pinning and responsible for the enhancement of the critical current density, doping improves the magnetic behavior of this material.

In this work we present a study performed on hot isostatic pressed samples of MgB_2 , irradiated with electrons, protons, and gammas, in order to create a significant number of de-

fect densities on the samples. The effect of irradiation was compared with pristine MgB_2 , prepared under the same conditions. The main motivation was to induce atomic disorder by means of different types of irradiation in order to quantify the pinning effects on the critical current.

2. Experimental results and discussion

The polycrystalline MgB_2 samples were prepared by the hot isostatically pressed method. This has been the most successful way to produce dense samples [3]. Four samples were used: the first three were irradiated with low flux doses of electrons, protons, and gamma rays; the fourth one was kept pristine, without any irradiation. The total irradiation doses absorbed by the samples were the following; electrons 5 MGy, gammas 5 MGy, and protons 244 MGy. The pristine material presents a transition temperature of 39 K. The irradiated samples show transition temperatures about one degree below 39 K. Measurements of M-H at different temperatures were performed using a MPMS Quantum Design magnetometer. The magnetization hysteresis loops were measured under magnetic fields up to 4 T, and the magnetic sweep rate was approximately of 0.3 T/min. Isothermal M-H curves presented many flux jump avalanches mainly at low temperature. As the temperature was increased, the jumps decrease in number and size. We measured the isothermal M-H loops at 2, 10, 15, 20 and 23 K, but for clarity we only show here results at 2 and 10 K in Figs. 3 and 4, respectively. However, we have to mention that the number of flux jumps is dramatically reduced as the temperature was increased. At high temperatures (20 and 23 K), only a few flux jumps still exist.

Figure 5 shows the applied magnetic field dependence of the critical current density (J_C) at $T = 2$ and 10 K, for non irradiated and irradiated samples. J_C was evaluated using Bean's model [17] and taking into consideration a parallelepiped shaped sample, measured with the longitudinal axis parallel to the field in order to reduce demagnetization effects. According to Bean's model, $J_C = 30\Delta M / (a - b^2/a)$, where ΔM (emu cm^{-3}) comes from magnetization hysteresis loop measurements, a and b are the dimensions in cm of the parallelepiped shaped sample, and J_C is given in A/cm^2 . At 2 K (upper panel Fig. 5), we observed that all samples display instabilities in the critical current, which are due to the high number of flux jump events, as was also seen in the hysteresis loops of Fig. 3. At zero magnetic field, the critical current density was about $1.09 \times 10^5 \text{ A/cm}^2$ for the pristine sample, while the gamma irradiated sample reaches a current density of about $8.72 \times 10^5 \text{ A/cm}^2$. At 10 K, J_C shows a radical change; it is more stable and only the irradiated samples with protons and electrons show jumps in J_C , below 1 T. The hysteresis loop at 10 K, Fig. 4, shows less flux instabilities which correspond to the stability of J_C . In Table I we present values for the current density at 2 and 10 K at zero magnetic field.

TABLE I. Critical current density (J_C) values at 2 and 10 K in zero applied field for MgB₂ dense samples.

Sample	J_C (A/cm ²)	J_C (A/cm ²)
	T=2 K, H=0	T=10 K, H=0
Non-irradiated	1.09×10^5	4.67×10^5
Protons	3.87×10^5	7.07×10^5
Electrons	1.93×10^5	9.54×10^4
Gammas	8.72×10^5	1.90×10^6

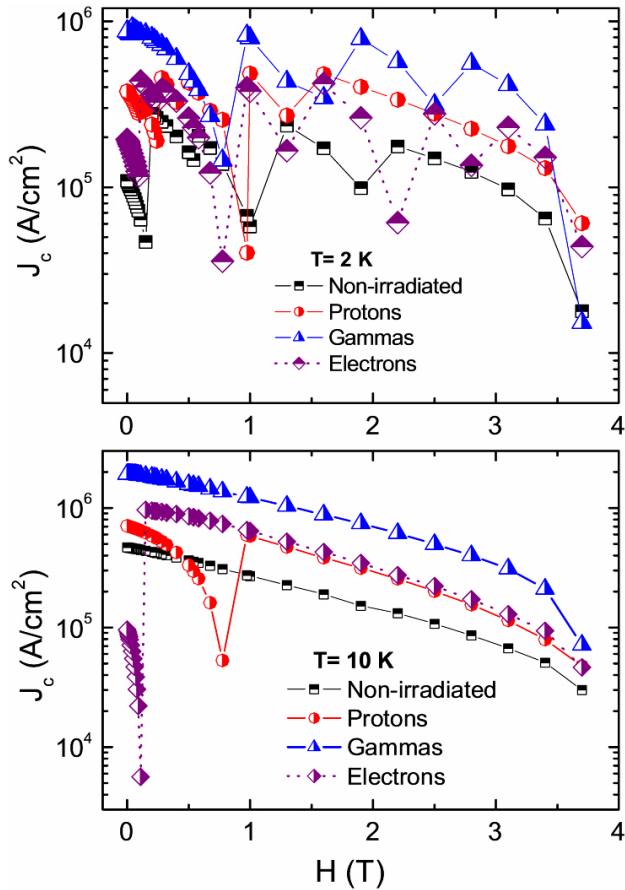


FIGURE 5. Critical current density (J_C) as a function of applied magnetic field (H) at 2 K (upper panel), and 10 K (lower panel) for MgB₂ dense samples, irradiated and non-irradiated.

As is well known, flux jump events have a negative effect on the critical current density in superconducting materials. At first glance, as might be normally expected, the maximum critical current must be reached at the minimum temperature and magnetic field. However, this is not the case: the reason for this is the influence of the high number of flux instabilities, as seen in Figs. 3 and 4, at 2 and 10 K, respectively. Another important result of this experiment is that the maximum current is obtained when the material is gamma irradiated; here, the magnitude of J_C is rather high as compared to the pristine sample and to the other irradiated samples. The maximum at 10 K is clearly related to the reduction of flux jump instabilities. This result reflects the strong pinning force, or in other words, the notable amount of lattice defects produced by the gamma irradiation when compared to proton and electron irradiation. This enhanced pinning force may be attributed to the energetic characteristic of gamma irradiation since this irradiation passes through the dense sample, while the damage is superficial with protons and electrons. Furthermore, the field dependence of J_C for the non-irradiated sample is lower than that for the irradiated samples. The difference observed in J_C - H curves should be attributed to the difference of the flux pinning effect on the samples. This drop of J_C strongly limits the performance of MgB₂ materials for applications.

3. Concluding remarks

This work presents a study of the effect of pinning and depinning on the flux jump vortices when samples are irradiated with electron, protons or gamma rays. We observed an increase in the critical current at low temperatures, when the flux jump instabilities are low in number. This effect is notably different when the samples are exposed to different types of irradiations. The gamma irradiated sample presented the best characteristics for the critical current densities due to the higher number of lattice defects created by the irradiation.

Acknowledgments

RE thanks DGAPA-UNAM for partial support of this work. The authors thank G. Guevara and F. Silvar, for their help in the preparation of this manuscript and for the helium supply.

1. C. Buzea and T. Yamashita, *Supercond. Sci. Technol.* **14** (2001) R115.
2. R. Escamilla *et al.*, *J. Phys.: Condens. Matter* **16** (2004) 5979.
3. J. Nagamatsu, N. Nakagawa, T. Muranaka, Y. Zenitani, and J. Akimitsu, *Nature* **410** (2001) 63.
4. J. Kortus, I.I. Manzin, K.D. Belashchenko, V.P. Antropov, and L.L. Boyer, *Phys. Rev. Lett.* **86** (2001) 4656.
5. J.M. An and W.E. Pickett, *Phys. Rev. Lett.* **86** (2001) 4366.
6. A.L. Ivanovskii, *Phys. Solid State* **45** (2003) 1829.
7. F. Bouquet *et al.*, *Europhys. Lett.* **56** (2001) 856.
8. R.S. Gonnelli *et al.*, *Phys. Rev. Lett.* **89** (2002) 247004.
9. A. Serquis *et al.*, *J. Appl. Phys.* **92** (2002) 351.
10. W.N. Kang, H.J. Kim, E.M. Choi, C.U. Jung, and S.I. Lee, *Science* **292** (2001) 1521.
11. S. Jin, H. Mavoori, C. Bower, and R.B. van Dover, *Nature* **411** (2001) 563.

12. V.V. Chabanenko *et al.*, *Supercond. Sci. Technol.* **11** (1998) 1181; V. Chabanenko *et al.*, *J. Low Temp. Phys.* **130** (2003) 175.
13. E. Altshuler and T.H. Johansen, *Rev. Mod. Phys.* **76** (2004) 471.
14. A.A. Golubov and I.I. Mazin, *Phys. Rev. B* **55** (1997) 15146.
15. A. Gurevich, *Phys. Rev. B* **67** (2003) 184515.
16. A.A. Golubov and A.E. Koshelev, *Phys. Rev. B* **68** (2003) 104503.
17. C.P. Bean, *Phys. Rev. Lett.* **8** (1962) 250; C.P. Bean, *Rev. Mod. Phys.* **36** (1964) 31.